Single-photon hot-electron ionization of C_{70}

Åke Andersson,[1] Luca Schio,[2] Robert Richter,[3] Michele Alagia,[2] Stefano Stranges,[2,4] Piero Ferrari,[5] Klavs Hansen,[6,7,*] and Vitali Zhaunerchyk[1,†]

[1]*Department of Physics, University of Gothenburg, 41296 Gothenburg, Sweden*
[2]*IOM-CNR Tasc, SS-14, Km 163.5 Area Science Park, Basovizza, 34149 Trieste, Italy*
[3]*Elettra - Sincrotrone Trieste, Area Science Park, 34149 Basovizza, Trieste, Italy*
[4]*Dipartimento di Chimica e Tecnologie del Farmaco, Universitá Roma La Sapienza, Rome 00185, Italy*
[5]*Quantum Solid-State Physics, Department of Physics and Astronomy, KU Leuven, 3001 Leuven, Belgium*
[6]*Lanzhou Center for Theoretical Physics, Key Laboratory of Theoretical Physics of Gansu Province and School of Physical Science and Technology, Lanzhou University, Lanzhou, Gansu 730000, China*
[7]*Center for Joint Quantum Studies and Department of Physics, School of Science, Tianjin University, 92 Weijin Road, Tianjin 300072, China*

(Received 16 October 2022; accepted 5 December 2022; published 6 January 2023)

Gas phase C_{70} molecules have been ionized with single photons of energies between 16 and 70 eV, and the electron spectra measured with velocity map imaging in coincidence with the ions. The doubly ionized and unfragmented species was present at photon energies of 22 eV and up, and triply charged ions were present from 55 eV. The low-kinetic-energy parts of the spectra are explained with thermal emission of transient hot electrons. We propose a generally applicable mechanism, named resonance ionization shadowing, for the creation of hot electrons by absorption of above-threshold energy photons.

DOI: 10.1103/PhysRevA.107.013103

I. INTRODUCTION

The large separation in timescales for electronic motion and vibrational motion of nuclei opens the possibility of an intermediate phase of transiently hot electrons in molecules and clusters. If present, this phase will exist between the time of the initial excitation of electrons and the dissipation of the energy into vibrational motion. It tends to be manifested particularly clearly in finite systems but has also been invoked in the description of the two-temperature model of solid surfaces exposed to short laser pulses [1].

In the gas-phase context it was introduced as the explanation of the Penning ionization yields of C_{60} and C_{70} in Ref. [2]. Soon after it was observed also to be present in C_{60} upon excitation with multiple low-energy photons from laser pulses with a duration around 100 fs [3], later confirmed with added quantum-mechanical calculations [4]. Subsequently, the phenomenon successfully explained ionization of sodium clusters with short-pulse laser light [5–7]. Following this development, it has been seen for a number of different systems excited with short laser pulses, including C_{70} [8] and a number of polycyclic aromatic hydrocarbon (PAH) molecules [9].

The dynamics of multielectron excited states involved in the phenomenon was considered theoretically with different approaches in Refs. [10–12], in addition to the more phenomenological models used to summarize the experimental results. An integral part of this modeling when applied to molecules or clusters is the dissipation of the incoherent electronic excitation energy in the hot-electron phase into the vibrational modes of the molecule. This coupling has been described in terms of a simple exponential decay of the excitation energy, involving a single parameter of dimension time, aptly named the coupling time. For some of the gas-phase molecules studied, a proxy for this electron-phonon dissipation time has been measured by pump-probe experiments [4,7,13]. In other cases it has been fitted from ion-yield curves for different clusters [14]. The values found range from a few hundred femtoseconds to a few picoseconds. The fastest dissipation occurs for C_{60}, with a time constant of 240 fs [14] or 400 $\pm$ 100 fs [4], and the slowest are the picosecond or longer times for sodium clusters [6]. Experiments performed on thin films of C_{70} have shown a very brief electron-electron equilibration time, undetermined but below the pulse duration of 165 fs used in these experiments [15]. The results in Ref. [4] suggest a lower limit of 10 fs for C_{60} from peaks shapes.

The initial electron equilibration in the creation of the hot-electron phase has received much less attention experimentally than the final, dissipation stage, although it is clearly of interest for the possibility of single-photon ionization of larger classes of molecules in, e.g., astrophysical contexts. In addition, studies of single-photon hot-electron ionization will give insight into the mechanisms of absorption and initial dissipation of the energy. Moreover, single-photon processes come with the very attractive feature that they eliminate the uncertainty in energy that accompanies multiphoton processes used previously for studies of the effect and have already given insights after the first observation reported in Ref. [16].

The clearest experimental signature for these purposes remains the emission of thermal electrons corresponding to the eV temperatures that characterize the hot-electron phase. The form of the thermal electron spectra is shaped by a number of factors [17]. The combined result of these is that for neutral and positively charged emitters, the energy distributions

*hansen@lzu.edu.cn, KlavsHansen@tju.edu.cn
†vitali.zhaunerchyk@physics.gu.se

resemble Boltzmann factors with the effective temperatures given by the product microcanonical electron temperature, as discussed in Refs. [18,19].

In addition to the Boltzmann-like shape of the spectrum, there are several other features that make it distinct from the spectra originating either from direct ionization or from thermal emission from completely equilibrated molecules, known as thermionic emission. A necessary feature of the spectra is that the velocity distributions of the emitted electrons must be spherically symmetric. Although this is a property shared with electrons emitted into single-particle *s* states, the two processes have different photon energy dependences, which makes them easy to distinguish. The thermionic emission mechanism produces significantly lower effective temperatures (see, e.g., the 3500 K (0.30 eV) values reported in Ref. [20], compared with the one-photon hot-electron ionization of C_{60} measured to 1.58 eV (18 300 K), reported in Ref. [16]). The other difference is the much longer timescale on which thermionic emission can be observed. Thermionic emission will, for low excitation energies, extend to several microseconds, producing a long tail on the mass peak in time-of-flight mass spectra [21], often accompanied by a substantial amount of fragmentation.

For the doubly ionized species observed in the experiments here, two other possible channels should be considered. One is the direct double-electron ionization. The electrons associated with prompt double ionization are characterized by a U-shaped electron kinetic-energy distribution [22]. The steepness of these distributions depends on the relation between photon energy and the double-ionization potential values.

Another possible channel is the emission of a second electron by regular thermionic emission. This process would occur after the excitation energy has been dissipated into the predominantly vibrationally excited equilibrium state. However, it is ruled out for two reasons. One is that the competing C_2 loss channel would dominate over thermionic emission by a large factor. The second is that delayed emission is absent in the time-of-flight mass spectra for the doubly charged species.

Apart from the initial Penning ionization study on C_{60} and C_{70} [2] and the one-photon hot-electron ionization study in Ref. [16], all of the experimental studies mentioned have been performed with short laser pulses of subthreshold photon energies. Although the competing direct (spectroscopic) ionization channel also appears prominently (see, e.g., Ref. [23] for a study of C_{60}), the study in Ref. [16] showed that absorption of high-energy photons by C_{60} can, indeed, give rise to a significant branching to hot-electron emission. It is, however, not obvious how general the single-photon hot-electron phase phenomenon is. The present experiment aims to answer whether it is also present for C_{70}.

II. EXPERIMENTAL AND THEORETICAL PROCEDURES AND RESULTS

The experiments were performed at the GasPhase beamline at the synchrotron ring Elettra. The procedures were similar to those used for C_{60} [16], and only a brief description will be given here. For further specifics of the beamline the reader is referred to Refs. [24,25]. The fullerene material was acquired from Sigma-Aldrich, with a purity of 98%. The sample was heated *in situ* for 5 days above 200 °C to outgas solvents and other volatile contaminants. During measurements the molecules were sublimed from an oven with an initial temperature of 430 °C that was slowly increased to 470 °C at the end of the run in order to keep the evaporation rate constant. The temperature was measured by a thermocouple attached to the oven. The linearly polarized light was filtered by standard filters at different wavelengths as needed.

The electron spectra were recorded on a single-count basis with a velocity-map-imaging (VMI) spectrometer equipped with a dual-delay line-position-sensitive detector and analyzed offline. The coincidence of electrons and ions was extracted offline from the recorded time of flight of the ions with an electron detection defining zero time. The detector allowed detection of only a single electron per event. To reduce the number of false coincidences, the light intensity was reduced to electron count rates of 11–18 kHz and ion count rates of 2–8 kHz. As the detection efficiency does not depend on the origin of an electron, the spectra of molecules with a specific charge state are equal-weight average spectra of all emitting charge states leading to the final state.

Spectra were recorded for photon energies of 16, 20, 22, 23.8, 26, 28, 30, 35, 40, 45, 50, 55, 60, 65, and 70 eV, always with the polarization parallel to the VMI detector plane. No tails on the mass spectra that would indicate a thermionic emission from a completely equilibrated system were observed in this experiment. Likewise, the substantial fragmentation that accompanies thermionic emission for fullerenes was absent in the C_{70} mass spectra recorded in this work, as in our previous work on C_{60} [16]. The raw-data spectra for the three lowest measured charge states of the unfragmented molecule at several selected photon energies are shown in Fig. 1.

The measured VMI spectra are the momentum distributions of the emitted electrons projected on the detector plane. On the VMI detector surface the required spherical symmetry of the hot electrons corresponds to a circular symmetry. Figure 2 shows the angular symmetry of the low-energy electrons and the contrast to the asymmetry for higher-energy electrons for a spectrum recorded after exposure to 20-eV photons. At low photon energies, the spectrum contains a wide base with structures that can be identified as features of direct ionization and hence of spectroscopic nature. The ions detected in coincidence with electrons with nearly zero kinetic energy, together with the appearance of the circular symmetry of these parts of the spectra, indicate the emergence of the hot-electron spectra. Indeed, for all photon energies the central, lowest-energy part of the spectra showed no sign of a correlation of the ion count with the direction of the light polarization, indicative of the required symmetrical distributions. The absence of any signal beyond the weak noise in Figs. 1(g) and 1(m)–1(p) demonstrates that the ionization depends on the photon energies and that any energy provided by the source is negligible. The energy limits defining the precise frames where the electron signal appears and disappears are discussed below.

With the chosen light polarization the complete three-dimensional distributions are obtained from the VMI spectra by deconvolution. The deconvolution was done with the inverse Abel transform as implemented in the MEVIR software

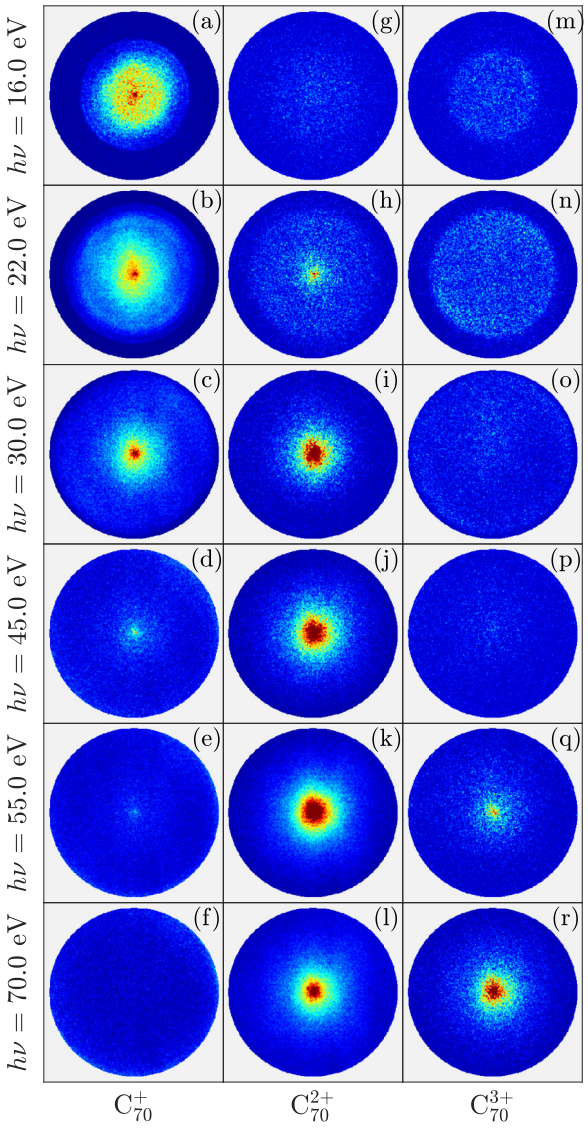

FIG. 1. The raw spectra of, from left to right, $C_{70}{}^{+}$, $C_{70}{}^{2+}$, and $C_{70}{}^{3+}$. The narrowing of the electron signal into a low-momentum peak in the $C_{70}{}^{+}$ column results from the transition of the ionization process from direct to hot-electron emission. As can be seen, the second ionized species is first visible at 22 eV, and the triply charged appears at 55 eV. The strong ion yield of the highly charged species contrasts with the result for C_{60}, for which the high-photon-energy spectra are dominated by the fragments.

[26]. Deconvolution of the spectra requires that the entire spectrum is projected onto the VMI detector surface. The highest electron energy for which this is guaranteed was 23 eV for the VMI voltages used in the experiment. This limits the photon energies to below 23 eV $+E_{i,1}$ for the singly ionized species, with $E_{i,1}$ being the first ionization energy. The value of $E_{i,1} = 7.4$ eV was measured in Ref. [27], making this limit equal to 30.4 eV. A conservative safety margin on the masking reduces the highest photon energy to 26 eV for the singly charged species.

As a check of the procedure, the value of the ionization energy can be inferred by tracing the position of the highest occupied molecular orbital (HOMO) band as a function of the

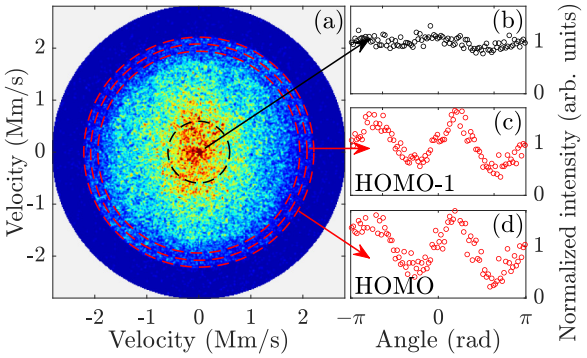

FIG. 2. A measured spectrum for C_{70} at the photon energy 20 eV. (a) shows electron intensities across the detector surface. (b) shows the angle-resolved intensities for the low-energy part of the spectrum, and two high-energy-electron parts defined by the red circles are shown in (c) and (d). The flat distribution in (b) is consistent with a spherically symmetric momentum distribution, in contrast to the direct-ionization electrons in (c) and (d). The shift of the curves in (c) and (d) relative to the zero angle is due to a corresponding rotation of the detector relative to the light polarization.

photon energy. The four photon energies from 16 to 23.8 eV can be used for that purpose. Figure 3 shows the trace used to determine $E_{i,1}$ on the deconvoluted VMI spectra. The value from this determination is 6.9 ± 0.5 eV, where the uncertainty is mainly due to the width of the peaks, i.e., consistent with the value from Ref. [27].

The electron detector can only assign a position and hence a transverse momentum to an event when it is hit by a single electron. As the detection efficiency is less than unity, it is, therefore nevertheless, still possible to detect spectra from double- and triple-ionization events. In these cases the spectra are sums of two spectra (for double ionization) or three spectra (for triple ionization) with equal weights. The sum of the two lowest ionization energies is 18.84 eV [28], and all the electrons originating from double-ionization events at photon

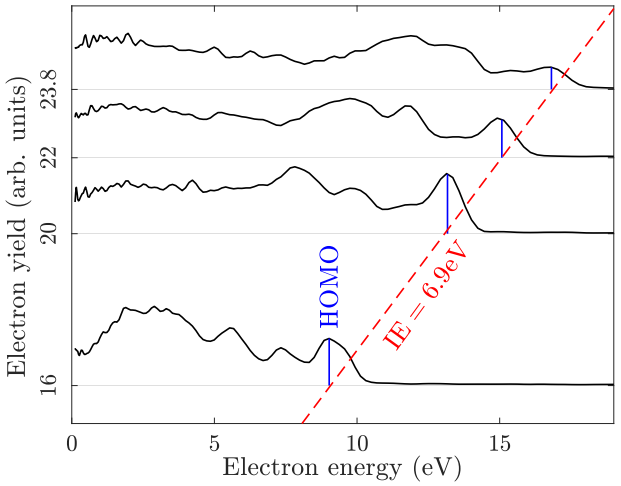

FIG. 3. The determination of the first ionization energy of C_{70} from the measured direct-ionization spectra. The photon energy at which each spectrum has been recorded is reported to the left of each baseline.

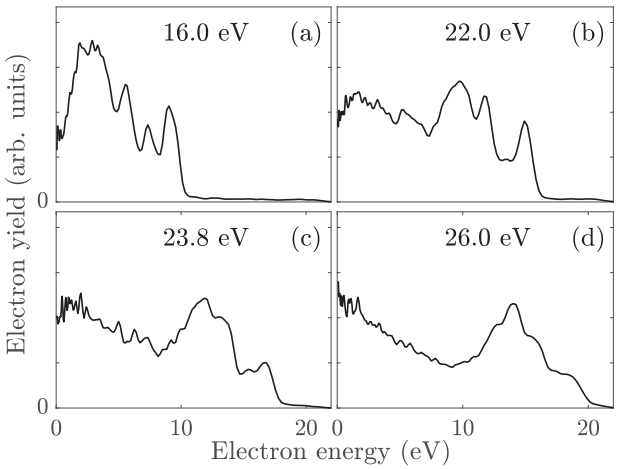

FIG. 4. The angular integrated electron spectra measured in coincidence with C_{70}^{+} for a series of photon energies. The $h\nu = 26$ eV spectrum is the highest measured spectrum that can be deconvoluted for singly ionized species. The direct-ionization yield, which for the $h\nu = 26$ eV spectrum is found between 10 and 20 eV, and the hot-electron signal, up to 10 eV, can be compared directly and are seen to be very similar at this photon energy.

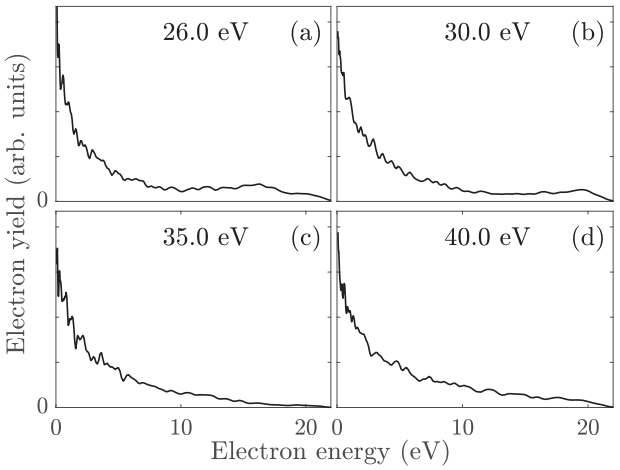

FIG. 5. The angular integrated electron spectra measured in coincidence with C_{70}^{2+} for the photon energies indicated in the panels.

energies below 40 eV are within detection range. For comparison, the value calculated with density-functional theory for the second ionization energy is 10.3 eV (see below for the method used). With the calculated single-ionization value of 7.3 eV this is in reasonable, albeit not perfect, agreement with the measured value. The high energy background is so low for the doubly ionized species that it is possible to deconvolute spectra up to the photon energy 45 eV. The appearance of the doubly charged ions at the photon energy $h\nu = 22$ eV is higher than the literature and theoretical values, as expected, and is consistent with the interpretation of the origin of the emitted electrons. In summary, inversion was performed for photon energies up to 26 eV for singly charged species and up to 45 eV for the doubly charged molecules and for the latter only for single-electron events.

The spectroscopic nature of the high-energy electrons is more apparent after deconvolution of the spectra. Figure 4, which shows deconvoluted spectra, demonstrates how this picture develops with increasing photon energy, in particular how the low-energy electrons become increasingly intense. Figure 5 shows the spectra of single electrons detected in coincidence with doubly charged ions. The potential competing process of the low-energy electrons by direct double ionization is not seen in the spectra in Fig. 5. These distributions would have a U shape, and the high-energy end of such a spectrum would be present at the high kinetic energies, which is clearly not the case. We can therefore rule out this channel as a significant contribution also the low-energy part of the spectra.

Quantum-chemical calculations of total and individual level energies were performed with density-functional theory (DFT) on C_{70} using the ORCA 5.1 software package [29]. For this, the Perdew-Burke-Ernzerhof functional [30] was used with the valence triple-zeta basis set with two sets of polarization functions (Def2-TZVPP) [31] and included atom-pairwise dispersion correction approximation to the DFT energy with Becke-Johnson damping (D3BJ) [32]. The geometries of both molecules were optimized for charge states 0, 1, and 2, and all the electrons were included in the calculation. Moreover, vibrational frequencies were computed, confirming that structures represent true minima on the potential-energy surface. In addition, single-point calculations of C_{60}^{q+1} and C_{70}^{q+1} on the optimized geometries of C_{60}^{q} and C_{70}^{q} were performed for $q = 0, 1, 2$ in order to calculate vertical first and second ionization energies.

Although the use of DFT to calculate the ionization energies and vibrational frequencies is well controlled, it is relevant to add a remark about the use of single-particle pseudostates to calculate level densities. These do not, in principle, give the single-particle states, nor do they guarantee that the single-particle approximation can be used. However, it is possible to compare level densities calculated with those states with the experimentally determined level density. A comparison was made in Ref. [14], where the two were found to agree very well. The only fit parameter used in that comparison was a single multiplicative constant. This provided the absolute magnitude, which cannot be extracted from the experiments. We will therefore use the same procedure here to calculate the level densities.

III. ANALYSIS AND DISCUSSION

Before a quantitative analysis of the deconvoluted spectra is presented, it is of interest to consider the raw data plot in Fig. 1 in some detail. Important features of the processes here and for C_{60} (see Fig. 1 of Ref. [33] and Fig. 5 of Ref. [16]) are as follows:

(i) The dominant open decay channel for the singly ionized C_{70}, shown in the second and third columns of Fig. 1, is further electron emission, producing the higher charge states of the molecules. For C_{60}^{+} fragmentation is somewhat more pronounced.

(ii) Intensities for C_{70}^{2+} (and for C_{70}^{3+}) appear at lower photon energy than the fragments of C_{60}^{+}.

(iii) The difference in appearance energies of the triply and doubly ionized charge states of C_{70} is much larger than the corresponding difference between the appearance energies of C_{58}^+ and C_{56}^+ from C_{60} [16].

Concerning feature (i), the tendency to ionize twice instead of causing fragmentation was already reported in Ref. [34]. A similar effect has been seen in naphthalene [35], where the relative intensities of doubly ionized species relative to singly charged fragments increase when photon energies are changed from 20.4 to 29.8 eV, in parallel with a strong suppression of fragmentation processes at the higher energies.

The explanation for feature (ii) is that the second ionization occurs from the hot-electron ensemble, whereas the fragmentation of C_{60}^+ ions occurs from the completely vibrationally thermalized ion. The difference in the heat capacity of the two emitting systems accounts for the main part of this difference in appearance energies. These aspects were already analyzed in detail in Refs. [14,16], where more quantitative details can be found. We note that also this observation is consistent with the hot-electron ionization mechanism.

The reason for the behavior in point (iii) is also the different natures of the decays of the two molecules. Addressing this question requires quantitative considerations of the appearance energies. For the C_{60} decay, the difference in the appearance energies of C_{58}^+ and C_{56}^+ is given mainly by the C_2 dissociation energy of C_{58}^+. This is seen with the following simplified, but still reasonably accurate, calculation. The appearance energy for fragment m in a decay chain can be calculated as the photon energy, which is the sum of the energies consumed in the previous decays plus the thermal energy needed for the mth decay. With an Arrhenius expression for the fragmentation rate constant we have

$$k(E) \sim \omega \exp(-D/T(E)), \tag{1}$$

with T being the effective microcanonical temperature at energy E and D being the evaporative activation energy. A linear relation between the (microcanonical) vibrational temperature T and the excitation energy E is assumed (E_m^{o} is the energy offset in this curve, and k_{B} is set to unity):

$$E = C_k T - E_m^{\mathrm{o}}. \tag{2}$$

With G defined as $\ln \omega t$ and t being the time of acceleration for the ion time of flight, this gives

$$h\nu_{\mathrm{appear},m} \approx D_m \frac{C_m}{G} + E_m^{\mathrm{o}} + \sum_{j=0}^{m-1} D_j - E_{\mathrm{source}}. \tag{3}$$

The last terms in the equation accounts for the energy consumption in the prior decays and the initial energy of the molecule. The small amounts of energy carried away by the C_2 fragments are ignored in the expression. When the contribution $D_m C_m/G + E_m^{\mathrm{o}}$ is approximately independent of m, the difference in the mth and $(m-1)$th appearance energies is

$$h\nu_{\mathrm{appear},m} - h\nu_{\mathrm{appear},m-1} \approx D_{m-1}. \tag{4}$$

This approximate identity of the sequential differences between appearance energies hinges on the similarity of the emission activation energies and the constancy of the heat capacity. These are expected to hold to a decent approximation for the C_2 loss activation energy and for the vibrational thermal properties. For the hot-electron emission processes seen for C_{70}, neither of these similarities will hold. The emission activation energies are the ionization energies, and their values increase with the charge state. Also the heat capacities vary with energy.

The estimate for the electron emission appearance energies goes as follows: The lowest effective temperature where hot-electron emissions occur is determined by the combination of the electron-vibrational cooling time and the electron-emission-rate constant using the relation

$$k(E) = 1/\tau. \tag{5}$$

We will set the coupling time to the C_{60} value of $\tau = 240$ fs measured in Ref. [14]. A slightly larger value of 400 ± 100 fs was fitted from the measurements reported in Ref. [4]. For smaller rate constants, dissipation into vibrational motion quenches the emission. The emission-rate constant for electrons is also written as an Arrhenius expression where the activation energy is the ionization energy E_{i}. The frequency factor is denoted by ω_{e}. Although the value of ω_{e} depends on the charge state, the dependence is minor and beyond the precision here, and the factor will therefore be set to the neutral molecule value. To find the temperature we use the caloric curve for a Fermi gas,

$$E = \frac{1}{2}\alpha T^2. \tag{6}$$

The initial electronic energy from the source can be set to zero.

The photon energy at which the second ionized species appears can then be calculated with the same logic as for the unimolecular decays, i.e., adding the consumed energies of the previous decays to the excitation energy calculated by Eq. (5). The result is

$$h\nu_2 = \frac{\alpha}{2(\ln \omega_{\mathrm{e}}\tau)^2} E_{\mathrm{i},2}^2 + E_{\mathrm{i},1} + \langle \varepsilon_{1,1} \rangle, \tag{7}$$

where $\langle \varepsilon_{1,1} \rangle$ is the average electron energy in the first ionization. By the same argument the triply ionized species appear at the photon energy

$$h\nu_3 = \frac{\alpha}{2(\ln \omega_{\mathrm{e}}\tau)^2} E_{\mathrm{i},3}^2 + E_{\mathrm{i},1} + E_{\mathrm{i},2} + \langle \varepsilon_{2,1} \rangle + \langle \varepsilon_{2,2} \rangle, \tag{8}$$

where $\langle \varepsilon_{2,1} \rangle$ and $\langle \varepsilon_{2,2} \rangle$ are the electron energies of the first and second emitted electrons in this process. These energies are larger than the counterpart for C_2 emission and cannot be ignored in the analysis for electron emission. The emission of the first electron occurs at different energies for the two processes, with different final charge states, and $\langle \varepsilon_{1,1} \rangle$ is therefore different from (smaller than) $\langle \varepsilon_{2,1} \rangle$. With a value of 26 eV for $h\nu_2$ (see Fig. 1), first ionization energy $E_{\mathrm{i},1} = 7.4$ eV, and second ionization energy $E_{\mathrm{i},2} = 11.4$ eV, the coefficient in Eq. (7) becomes

$$\frac{\alpha}{2(\ln \omega_{\mathrm{e}}\tau)^2} = \frac{h\nu_2 - E_{\mathrm{i},1} - \langle \varepsilon_{1,1} \rangle}{E_{\mathrm{i},2}^2} = 0.13\,\mathrm{eV}^{-1} \tag{9}$$

when we use the value $\langle \varepsilon_{1,1} \rangle = 2$ eV. This result is compared below with the theoretical value derived from the rate constant after that calculation has been made.

Using the close similarity of the first two ionization energies to those of C_{60}, 7.6 and 11.4 eV, respectively, we adopt the third ionization energy of C_{60}, $E_{i,3} = 16.6$ eV, for C_{70}. This predicts an appearance photon energy of the third ionized molecule of

$$h\nu_3 = (18.8 + 5)\,\mathrm{eV} + 0.13\,\mathrm{eV}^{-1}(16.6\,\mathrm{eV})^2 = 60\,\mathrm{eV}, \quad (10)$$

where by inspection of the measured spectra shown in Fig. 5 we estimated the sum $\langle\varepsilon_{2,1}\rangle + \langle\varepsilon_{2,2}\rangle$ to be 5 eV. The estimated uncertainty on $h\nu_3$ is 9 eV. The experimental value of this crossover photon energy is more uncertain than $h\nu_2$, but the calculated value is within the range of the possible experimental values that lie between 45 and 60 eV.

For the above analysis a description in terms of a Fermi gas is sufficient, but for a more precise description and an assessment of the value of α, a more accurate calculation of the thermal properties of the hot electrons is required. The relevant thermal properties are the level densities, or density of states and rate constants. They are calculated with the method given in the Appendix of Ref. [14]. The input data are the energy levels from the DFT calculation of the energies. As the temperature is the microcanonical version, we use the value derived from the level density ρ [18],

$$\frac{d\ln\rho(E)}{dE} = T^{-1}. \quad (11)$$

As k_B is set to unity, temperatures are therefore given in eV. This calculation for the singly charged molecule essentially confirms the Fermi gas ansatz, albeit with an offset in the temperature. The fitted form is

$$E = \frac{1}{2}\alpha'\left(T^2 - T_0^2\right), \quad (12)$$

with $\alpha' = 46$ eV^{-1} and $T_0^2 = 0.3$ eV^2. These values pertain to the singly charged molecule, but the values for the other charge states are similar. As a side remark we note that the offset in the caloric curve is analogous to the similar and well-documented offset that appears in the caloric curve of quantized vibrational motion. The interpretation of the offset here is different, and the value cannot be ascribed to a zero-point motion like for the vibrations. The offset in temperature prevents a comparison of α' fitted here and α calculated from Eq. (9) with the rate constant in Eq. (13). This comparison will be made below.

The kinetic-energy-resolved electron-emission-rate constant is given by the expression [14]

$$k^{(q)}(E,\varepsilon)d\varepsilon = \frac{2m_e\sigma(\varepsilon)}{\pi^2\hbar^3}\varepsilon\frac{\rho^{(q+1)}(E - E_{i,q} - \varepsilon)}{\rho^{(q)}(E)}d\varepsilon. \quad (13)$$

Here ε is the kinetic energy of the electron, m_e is the mass of the electron, $\rho^{(q)}(E)$ is the level density of the charge state q at energy E, and $E_{i,q}$ is the ionization energy. The factor of 2 in Eq. (13) is the spin degeneracy of the electron, and $\sigma(\varepsilon)$ is the capture cross section for an electron in the Coulomb potential of the decay product. To find the relevant rate constant, the kinetic energy is integrated over:

$$k^{(q)}(E) \equiv \int_0^E k^{(q)}(E,\varepsilon)d\varepsilon. \quad (14)$$

The numerically integrated function is shown in Fig. 6.

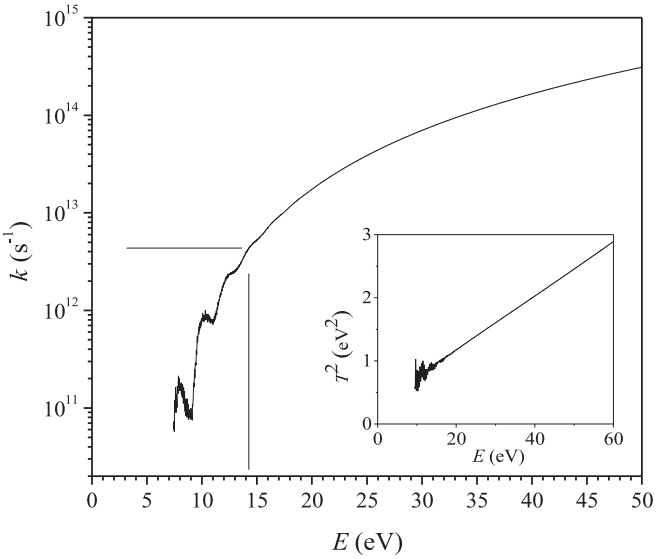

FIG. 6. The rate constant for emission of the second electron. The reciprocal coupling time and the corresponding lower limit of the energy of an emitting molecule are indicated by the horizontal and vertical lines. The inset shows the square of the microcanonical electron temperature v. excitation energy. This is clearly very well represented by Eq. (12).

With Eq. (13) we can describe the kinetic-energy distributions with the function

$$P(\varepsilon;E,q)d\varepsilon = \sigma(\varepsilon)\varepsilon\rho^{(q+1)}(E - \varepsilon)d\varepsilon. \quad (15)$$

For the capture cross section the classical values used are

$$\sigma(\varepsilon) = \pi r_0^2\left(1 - \frac{V(r_0)}{\varepsilon}\right) \quad (16)$$

and

$$V(r_0) = -\frac{(q+1)e^2}{4\pi\varepsilon_0 r_0} = -(q+1)3.0\,\mathrm{eV}. \quad (17)$$

$r_0 = 5.3$ Å is the (angle-averaged) radius of the electron distribution in the molecule based on the bulk density of 1.64 g/cm^3 [36] and a fcc packing ratio of 0.74 [37]. The level densities can be approximated as

$$\rho^{(q+1)}(E - \varepsilon) \approx \rho^{(q+1)}(E)\mathrm{e}^{-\varepsilon/T(E)}. \quad (18)$$

At a given photon energy the energies of the emitting ions are

$$E_1 = h\nu - E_{i,1} \quad (19)$$

for the first emitted electron and

$$E_2 = h\nu - E_{i,1} - E_{i,2} - T(E_1) \quad (20)$$

for the second. $T(E_1)$ is the average value of the energy carried away by the electron during the first ionization. The temperatures are then found from Eq. (12), which can be used for both charge states. Denoting these temperatures by T_1 and T_2, the spectra become

$$P(\varepsilon) \propto \frac{(\varepsilon + 3.0\,\mathrm{eV})\,\mathrm{e}^{-\varepsilon/T_1}}{T_1(T_1 + 3.0\,\mathrm{eV})} + \frac{(\varepsilon + 6.0\,\mathrm{eV})\,\mathrm{e}^{-\varepsilon/T_2}}{T_2(T_2 + 6.0\,\mathrm{eV})}. \quad (21)$$

Given the fairly high temperatures, the term proportional to ε is needed here.

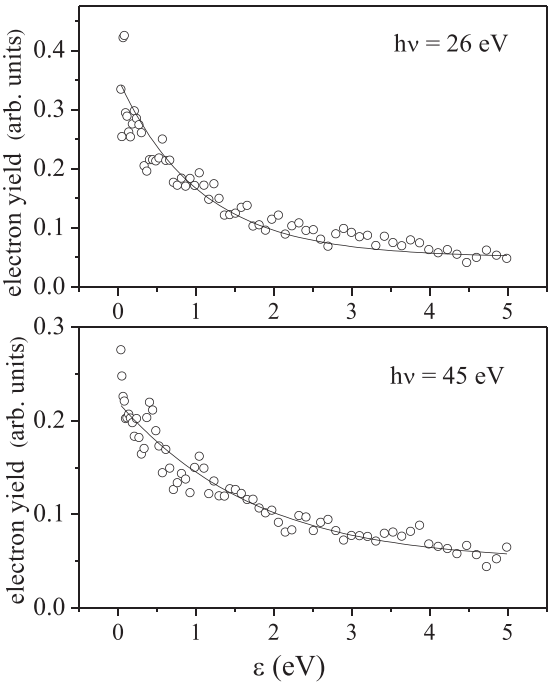

FIG. 7. The low-energy parts of the experimental doubly ionized spectra (open circles) and the predicted biexponential decay in Eq. (21) with temperatures of 1.053 and 0.753 eV for the $h\nu = 26$ eV curve and 1.391 and 1.174 eV for the $h\nu = 45$ eV curve, given by Eq. (12) and calculated with the energies as described in the main text.

The two temperatures in Eq. (21) are theoretically rather similar in the photon energy range from 26 to 45 eV. The values of T_1 and T_2 for $h\nu = 26$ eV, for example, which give rise to the largest difference, are 1.05 and 0.75 eV. For $h\nu = 45$ eV they are 1.39 eV and 1.17 eV. This makes a direct fit uncertain. A compounding complication for a fit is that the spectra are found to contain a small and broad background. Instead, the theoretical curves are plotted with a constant offset of 0.05. They are shown in Fig. 7 for the lowest and highest photon energies for spectra of doubly ionized molecules. The quality of the prediction for the spectra of the four photon energies not shown is very similar.

With the expression for the rate constant we check the consistency of the hot-electron picture by comparing the theory value α' with the experimental value α on the right-hand side of Eq. (9). The rate constant to choose is the one corresponding to the time constant of dissipation of the electronic excitation energy into vibrational motion, Eq. (5): $k(E) = 1/240$ fs. This gives an energy of 13 eV. Using this for the first ionization gives the corresponding singly ionized version of Eq. (9):

$$\frac{\alpha}{2(\ln \omega_e \tau)^2} = \frac{13\ \text{eV}}{E_{i,1}} = 0.10\,\text{eV}^{-1}, \tag{22}$$

which is in reasonable agreement with the experimental value of 0.13 eV^{-1}. We take this as a confirmation of the values used. It should be noted that, clearly, this confirms only the product of the electron-emission frequency factor and the value of τ and not the values of the two quantities separately.

Finally, we address the question of the initial excitation of the molecule. One of the challenges still facing the description of the phenomenon is an explanation of the mechanism of the initial excitation. A part of this question, which will be susceptible to future experiments and that has obvious implications for the kinetic energies of the emitted electrons, is the branching ratio between direct and hot electron ionization. A full quantum-mechanical description of the dynamics of the process is beyond the scope of this paper, but we will suggest a possible mechanism which will convert a single-particle excitation into multielectron excitation and hence provide the initial energy dissipation needed to produce the electron spectra seen in this work.

The suggested description builds on the single-electron picture. In the initial reaction, the photon is absorbed by a single electron which is promoted to a vacuum state, converting all energy in excess of the binding energy E_b to kinetic energy according to the standard relation

$$E_k = h\nu - E_b. \tag{23}$$

After this, the electron starts to move across the fullerene. The time it takes for this crossing is given classically by

$$t_c \sim \frac{2r_0}{\sqrt{2(h\nu - E_b)/m}}. \tag{24}$$

During this motion the remaining valence electrons will be exposed to the electric field of the excited electron. This will excite the surface plasmon resonance with some probability, which depends on the speed of the emitted electron. Setting t_c to half the period of a resonance, the departing electron will then be in resonance with an excitation with a quantum energy of

$$\hbar\omega = \hbar\pi\sqrt{2(h\nu - E_b)/m}/2r_0. \tag{25}$$

A kinetic energy of 50 eV, for example, will give a value of 8.6 eV for the right-hand side and will be optimal for exciting an oscillation around that energy. This energy is on the order of the peak energy of the surface plasmon resonance, which is located with a centroid energy of $\hbar\omega \approx 20$ eV and, significantly, with a width of similar magnitude [38]. Electron-energy-loss spectroscopy shows a strong absorption of a collective nature from 5-eV electron energy and up [39], similar to the optical cross section. The attenuation length was given for C_{60} films in Ref. [40] for a single energy. The value compares well with values from intercalated fullerite samples, and the pure fullerite attenuation length at the energies relevant here can be taken with some confidence to be around the size of the molecule. There is little reason to believe that the value for C_{70} is significantly different, given the similar spectra in Ref. [39]. These experimental indications suggest that excitation by the prescribed mechanism is, indeed, likely to occur.

Leaving aside the precise value of the matrix element for exciting the plasmon resonance, it is also clear that at least the timescales match semiclassically. Moreover, as this resonance is a collective motion of a large number of electrons, with the number reflected in the large oscillator strength, a coupling to it will deposit the kinetic energy into a large number of valence electrons, facilitating the dissipation into incoherent energy which is the hallmark of the hot-electron phase.

The mechanism suggested here has some support in the ionization of metal clusters. In Ref. [41] ionization yields of alkali-metal clusters were reported. The data show reductions in ionization yields above the surface plasmon resonance. This was discussed qualitatively in terms of a mechanism that couple photoelectrons and the plasmon, similar to the one predicted here. In particular, it will impact measured ionization cross sections, such as those reported in Ref. [38], although for those measurements the corrections will mainly occur on the high-energy side of the peak value. An experimental signature of the effect is a reduced direct-ionization efficiency and an increased amount of hot-electron ionization in the energy region where the kinetic energy in the initial stage is conducive to excitation of the resonance, i.e., fulfills Eq. (25). This is effectively a shadow of the plasmon resonance. This resonance ionization shadowing must be expected to be present in other clusters or molecules that have large oscillator strength resonances. The precise parameters of the effect, such as the branching ratio of direct ionization to hot-electron formation, will depend on the centroid energy, its width, and, to some extent, also its oscillator strength. The molecular geometry may likewise determine the initial coupling to the resonance.

IV. CONCLUSION AND OUTLOOK

We have measured the single-photon hot-electron ionization of C_{70}. It shows the same main features as the process for C_{60}, albeit with a somewhat stronger yield of the doubly ionized species compared to fragmentation. The measurements thus demonstrate that the mechanism is not restricted to a single fullerene. The mechanism by which the molecules absorb a photon with energy above the ionization energy and equilibrate it is not yet established. In this work we have suggested a mechanism involving excitation of the surface plasmon by a departing electron. This mechanism should be fairly general. If correct, it will suppress the ionization as a function of photon energy in a wide energy region, usually above the plasmon centroid. Part of the suppression will be compensated by the enhanced hot-electron emission. The suggested mechanism is not a direct excitation of the plasmon and explains that the onset of the hot-electron emission appears above its centroid energy, as already seen for C_{60}. Hence, contrary to previous statements, the surface plasmon is relevant after all, albeit only indirectly.

ACKNOWLEDGMENTS

K.H. acknowledges support from NSFC with Grant No. 12047501 and from the 111 Project of the Ministry of Science and Technology of the People's Republic of China under Grant No. B20063 and thanks Y. Gong for advice on the presentation. P.F. acknowledges the Research Foundation Flanders (FWO) for a senior postdoctoral grant. The computational resources and services used in this work were provided by the VSC (Flemish Supercomputer Center), funded by the FWO and the Flemish government. We acknowledge Elettra Sincrotrone Trieste for providing access to its synchrotron radiation facilities. The authors also acknowledge the open access contribution of the Research Infrastructure (RI) Elettra. Comments from V. Kresin are gratefully acknowledged.

[1] S. I. Anisimov, B. L. Kapeliovich, and T. L. Perel'man, JETP **39**, 375 (1974).
[2] J. M. Weber, K. Hansen, M. W. Ruf, and H. Hotop, Chem. Phys. **239**, 271 (1998).
[3] E. E. B. Campbell, K. Hansen, K. Hoffmann, G. Korn, M. Tchaplyguine, M. Wittmann, and I. V. Hertel, Phys. Rev. Lett. **84**, 2128 (2000).
[4] S. Usenko, M. Schüler, A. Azima, M. Jakob, L. L. Lazzarino, Y. Pavlyukh, A. Przystawik, M. Drescher, T. Laarmann, and J. Berakda, New J. Phys. **18**, 113055 (2016).
[5] R. Schlipper, R. Kusche, B. v. Issendorff, and H. Haberland, Appl. Phys. A **72**, 255 (2001).
[6] M. Maier, M. Schätzel, G. Wrigge, M. Astruc Hoffmann, P. Didier, and B. von Issendorff, Int. J. Mass Spectrom. **252**, 157 (2006).
[7] M. Maier, G. Wrigge, M. A. Hoffmann, P. Didier, and B. von Issendorff, Phys. Rev. Lett. **96**, 117405 (2006).
[8] M. Kjellberg, O. Johansson, F. Jonsson, A. V. Bulgakov, C. Bordas, E. E. B. Campbell, and K. Hansen, Phys. Rev. A **81**, 023202 (2010).
[9] M. Kjellberg, A. V. Bulgakov, M. Goto, O. Johansson, and K. Hansen, J. Chem. Phys. **133**, 074308 (2010).
[10] V. V. Flambaum, A. A. Gribakina, G. F. Gribakin, and C. Harabati, Phys. Rev. A **66**, 012713 (2002).
[11] G. Gribakin and S. Sahoo, J. Phys. B **36**, 3349 (2003).
[12] J. Heraud, M. Vincendon, P.-G. Reinhard, P. M. Dinh, and E. Suraud, Eur. Phys. J. D **75**, 121 (2021).
[13] E. E. B. Campbell, K. Hansen, M. Hedén, M. Kjellberg, and A.V. Bulgakov, Photochem. Photobiol. Sci. **5**, 1183 (2006).
[14] K. Hansen, K. Hoffmann, and E. E. B. Campbell, J. Chem. Phys. **119**, 2513 (2003).
[15] W. Cong-fang, A. Xi-cheng, X. Zong-ju, Z. Ying-hua, Q. Jiang, and Q. Shi-xiong, Chin. Phys. Lett. **13**, 668 (1996).
[16] K. Hansen, R. Richter, M. Alagia, S. Stranges, L. Schio, P. Salén, V. Yatsyna, R. Feifel, and V. Zhaunerchyk, Phys. Rev. Lett. **118**, 103001 (2017).
[17] J. U. Andersen, E. Bonderup, and K. Hansen, J. Phys. B **35**, R1 (2002).
[18] J. U. Andersen, E. Bonderup, and K. Hansen, J. Chem. Phys. **114**, 6518 (2001).
[19] K. Hansen, *Statistical Physics of Nanoparticles in the Gas Phase*, Springer Series on Atomic, Optical, and Plasma Physics Vol. 73 (Springer, Dordrecht, 2018).
[20] F. Lépine and C. Bordas, Phys. Rev. A **69**, 053201 (2004).
[21] G. Walder and O. Echt, Int. J. Mod. Phys. B **06**, 3881 (1992).
[22] J. Andersson, S. Zagorodskikh, A. Hult Roos, O. Talaee, R. J. Squibb, D. Koulentianos, M. Wallner, V. Zhaunerchyk, R. Singh, J. H. D. Eland, J. M. Rost, and R. Feifel, Sci. Rep. **9**, 17883 (2019).
[23] H. R. Hrodmarsson, G. A. Garcia, H. Linnartz, and L. Nahon, Phys. Chem. Chem. Phys. **22**, 13880 (2020).
[24] R. R. Blyth, R. Delaunay, M. Zitnik, J. Krempasky, R. Krempaska, J. Slezak, K. C. Prince, R. Richter, M. Vondracek, R. Camilloni *et al.*, J. Electron Spectrosc. Relat. Phenom. **101–103**, 959 (1999).

[25] P. O'Keeffe, P. Bolognesi, M. Coreno, A. Moise, R. Richter, G. Cautero, L. Stebel, R. Sergo, L. Pravica, Y. Ovcharenko *et al.*, Rev. Sci. Instrum. **82**, 033109 (2011).
[26] B. Dick, Phys. Chem. Chem. Phys. **16**, 570 (2014).
[27] O. V. Boltalina, I. N. Ioffe, L. N. Sidorov, G. Seifert, and K. Vietze, J. Am. Chem. Soc. **122**, 9745 (2000).
[28] H. Steger, J. de Vries, B. Kamke, W. Kamke, and T. Drewello, Chem. Phys. Lett. **194**, 452 (1992).
[29] F. Neese, F. Wennmohs, U. Becker, and C. Riplinger, J. Chem. Phys. **152**, 224108 (2020).
[30] B. Hammer, L. B. Hansen, and J. K. Nørskov, Phys. Rev. B **59**, 7413 (1999).
[31] F. Weigend and R. Ahlrichs, Phys. Chem. Chem. Phys. **7**, 3297 (2005).
[32] S. Grimme, S. Ehrlich, and L. Goerigk, J. Comp. Chem. **32**, 1456 (2011).
[33] A. Reinköster, S. Korica, J. Viefhaus, K. Godehusen, O. Schwartzkopf, M. Mast, and U. Becker, J. Phys. B **37**, 2135 (2004).
[34] K. Mitsuke, H. Katayanagi, B. P. Kafle, C. Huang, H. Yagi, M. S. I. Prodhan, and Y. Kubozono, J. Phys. Chem. A **111**, 8336 (2007).
[35] G. Reitsma, J. Hummert, J. Dura, V. Loriot, M. J. J. Vrakking, F. Lépine, and O. Kornilov, J. Phys. Chem. A **123**, 3068 (2019).
[36] A. A. Kolomenskii, M. Szabadi, and P. Hess, Appl. Surf. Sci. **86**, 591 (1995).
[37] N. W. Ashcroft and N. D. Mermin, *Solid State Physics* (Saunders College Publishing, Philadelphia, 1976).
[38] I. V. Hertel, H. Steger, J. de Vries, B. Weisser, C. Menzel, B. Kamke, and W. Kamke, Phys. Rev. Lett. **68**, 784 (1992).
[39] E. Sohmen, J. Fink, and W. Krätschmer, Z. Phys. B **86**, 87 (1992).
[40] H.-N. Li, X.-X. Wang, and W.-F. Ding, J. Electron Spectrosc. Relat. Phenom. **153**, 96 (2006).
[41] K. Wong, V. Kasperovich, G. Tikhonov, and V. V. Kresin, Appl. Phys. B **73**, 407 (2001).